metals

MDPI

Article

The Microstructures of TiC–Ti_5Si_3-Reinforced Cu Matrix Composites Prepared by Ti–SiC Reaction

Chaoxian Zhang [1,2,3], Xiao Zhang [1,2,3], Wenzhi Miao [1,2,3], Jiangmin Wu [1,2,3], Fugong Qi [1,2,3], Jiyu Zhou [1,2,3] and Haimin Ding [1,2,3,*]

[1] School of Energy, Power and Mechanical Engineering, North China Electric Power University, Baoding 071003, China
[2] Hebei Key Laboratory of Electric Machinery Health Maintenance & Failure Prevention, School of Energy, Power and Mechanical Engineering, North China Electric Power University, Baoding 071003, China
[3] Hebei Engineering Research Center for Advanced Manufacturing & Intelligent Operation and Maintenance of Electric Power Machinery, North China Electric Power University, Baoding 071003, China
* Correspondence: dinghaimin@ncepu.edu.cn; Tel.: +86-(312)-7525404

Abstract: In this work, the TiC and Ti_5Si_3-reinforced Cu matrix composites with different contents were successfully prepared through Ti–SiC reaction in Cu melts; accordingly, the microstructures of them were studied, and the hardness of the composites was tested. It is found that the synthesized TiC are granular, with a size ranging from 0.5 μm to 3 μm, while the Ti_5Si_3 are rod-like hexagonal prisms with a diameter of about 1 μm and a length-to-diameter ratio of about 5~25. In addition, it is noticed that many Ti_5Si_3 rods are actually Cu@Ti_5Si_3 core–shell structure rods. TiC and Ti_5Si_3 alternately distribute in the Cu matrix to form the hybrid reinforcement system. With the increase in Ti–SiC content, the TiC particles, Ti_5Si_3 rods and Cu@Ti_5Si_3 increased obviously, and the solid skeleton structure of TiC–Ti_5Si_3 was formed. The hardness of the composites was 2.2 to 2.74 times greater than that of the as-cast pure copper. It is deduced that, compared to the composites reinforced by either TiC or Ti_5Si_3, the formation of the TiC–Ti_5Si_3 hybrid system is more helpful for improving the properties of the composites due to the different morphologies of TiC and Ti_5Si_3.

Keywords: Ti–SiC system; reactive wetting; hybrid reinforcement; hardness

Citation: Zhang, C.; Zhang, X.; Miao, W.; Wu, J.; Qi, F.; Zhou, J.; Ding, H. The Microstructures of TiC–Ti_5Si_3-Reinforced Cu Matrix Composites Prepared by Ti–SiC Reaction. *Metals* **2023**, *13*, 607. https://doi.org/10.3390/met13030607

Academic Editor: Ruslan R. Balokhonov

Received: 13 February 2023
Revised: 6 March 2023
Accepted: 10 March 2023
Published: 17 March 2023

1. Introduction

Cu has been widely used in the fields of electronics, functional materials, automobiles and machinery manufacturing because of its highly electrical nature, excellent conductivity, thermal conductivity and low cost (compared with Ag and Au) [1,2]. Recently, with the development of technology, the related industries have put forward higher requirements for the performance of copper. However, due to its poor strength, low hardness and wear resistance, the application of Cu in the industrial field is limited [3–6]. Developing novel Cu composites simultaneously characterized by excellent mechanical, tribological and corrosion properties has been the relevant challenge in materials science. In order to solve this problem, the main methods generally include macro- and micro-doping of alloys and the formation of special types of the structure (duplex, ultrafine, nanocrystalline, etc.), of which the reinforcement of Cu alloys by hard phases is widely used [7–9]. Table 1 shows the mechanical properties of Cu based composites with different reinforcements. It has been found that ceramic particles with excellent mechanical properties are usually introduced into the copper matrix as reinforcement phases, and copper can give full play to excellent comprehensive properties by regulating the type, content and distribution of the reinforcement phases [10–12]. However, due to poor wettability, it is generally difficult for ceramic particles to be effectively introduced into Cu melt [13–15]. For the time being, many methods have been developed for preparing the composite materials, and as a commonly used method, the reinforcement of composite materials can be in

situ synthesized in copper melt by the melt reaction method so as to realize the effective combination of the reinforcement and matrix interface and improve the properties of composite materials [16–19].

Table 1. Properties parameters of the reinforcement copper matrix composite [2].

Composites	1.6 vol.% GNP-Cu	18 vol.% TiB_2-Cu	15 vol.% β-Si_3N_4-Cu	10.68 wt.% TiC-Cu
Hardness	81 HV	128 HV	80.9 HV	105 HV

In Cu alloys, a large number of transition metal silicides tend to grow into rods with a certain aspect ratio, and the transition metal carbides are mostly granular. When both are used as reinforcers in the Cu matrix, they will work well together [19,20]. In our previous studies, it was found that Ti_5Si_3 will assist the introduction of TiC into Cu melts and promote its dispersion so that the TiC–Ti_5Si_3-reinforced Cu matrix composites have better distribution and organization than single TiC-reinforced composites [21–23]. It can be deduced that, compared to the composites reinforced by either TiC or Ti_5Si_3, the formation of a TiC–Ti_5Si_3 hybrid system is more helpful for improving the properties of the composites due to the different reinforcement morphologies of TiC and Ti_5Si_3.

At present, for the preparation of the TiC–Ti_5Si_3-reinforced Cu matrix composites, compared to the easy formation of Ti_5Si_3 by introducing Si and Ti elements into Cu melts, it is very difficult to add or synthesize TiC because of the poor wettability between the Cu melts and both TiC and other carbon-containing sources, such as graphite, which can react with Ti to form the TiC. As a consequence, the key aspect for preparing the TiC–Ti_5Si_3 hybrid-reinforced Cu matrix composites is how to introduce or synthesize TiC in the Cu matrix effectively. According to our previous works [21], it is also discovered that the reactive wetting based on the Ti–C reaction is a very effective way to prepare TiC-reinforced Cu matrix composites. Interestingly, when the carbon source is SiC in the Ti–C reaction system, besides the synthesis of TiC, Ti_5Si_3 can also be simultaneously formed. As a result, TiC–Ti_5Si_3 hybrid-reinforced Cu matrix composites can be prepared based on this.

It has been reported in our previous works [23,24] that the possible Ti–SiC reaction should be the following reaction (1). However, according to the formation of graphite derived from SiC during the reaction between Ti and SiC with a larger size, it has been suggested that there are two stages for the reaction (1): the first stage is forming Ti_5Si_3 and C; (2) the second stage is forming TiC. The reaction processes are expressed by reactions (2) and (3). According to the results, the simultaneous synthesis of TiC and Ti_5Si_3 by the addition of the Ti–SiC mixture into Cu melts is chosen as the method for preparing the TiC–Ti_5Si_3 hybrid-reinforced Cu matrix composites in this work.

$$SiC + Ti \rightarrow TiC + Ti_5Si_3 \quad (1)$$

$$SiC + Ti \rightarrow Ti_5Si_3 + C \quad (2)$$

$$Ti + C \rightarrow TiC \quad (3)$$

The Gibbs free energies for the above three reactions at 1273 K were calculated, which were about −909 kJ/mol, −400 kJ/mol and −170 kJ/mol, respectively. The calculated results prove that the reactions are thermally favorable.

Therefore, in this paper, in order to further investigate TiC–Ti_5Si_3-reinforced Cu matrix composites, based on the melt reaction method combined with the traditional casting process, Cu matrix composites with different contents of TiC–Ti_5Si_3 hybrid-reinforced phases were prepared, the microstructures of the prepared composites were analyzed and the hardness of the composites was also tested.

2. Experiment

The experimental procedure mainly includes the raw material preparation, the melt reaction, the sample preparation and analyses of the microstructures and compositions of the phases in the samples. During the preparation processes, Ti powder (30 μm), 6H-SiC powder (5 μm) and highly purified (99.9%) electrolytic Cu were used as the starting materials. At first, the Ti and SiC powders were uniformly mixed and then cold-pressed into compacts at room temperature. After that, the Ti–SiC compact was added into Cu melts melted by a high-frequency induction heating furnace at about 1250 °C. Finally, after holding for about 2 min, the melts were poured into graphite molds to obtain the samples.

The specimens were then cut from the prepared composites to carry out grinding and polishing through standard routines. The microstructures of the prepared as-cast samples were then analyzed by a scanning electron microscope (SEM) equipped with an energy dispersive X-ray spectroscope (EDS). In addition, in order to better examine the morphologies of the reaction products, an electrolytic etching method was applied to remove Cu from the surface of the samples through deep etching to expose the synthesized phases by placing the samples in the 18% phosphoric acid solution. In addition, the reaction products were also extracted from the as-cast composites, and the Cu matrix was completely etched off by means of the etching solution. The obtained electrolytic deep etching samples and the extracted powder were then investigated by SEM and XRD. In this work, the hardness of the samples was measured by a digital micro hardness tester using a load of 0.5 kgf. For each sample, hardness tests were repeated 10 times, and the average of those data was regarded as the hardness of the samples.

3. Results and Discussion

In this study, three kinds of prepared composites, with compositions of Cu-4.86Ti-1Si-0.43C, Cu-6.8Ti-1.4Si-0.6C and Cu-9.72Ti-2Si-0.86C, were prepared, which correspond to Cu-4.86Ti-1.43SiC, Cu-6.8Ti-2SiC and Cu-9.72Ti-2.86SiC, respectively, before the Ti–SiC reaction. In theory, when SiC absolutely reacts with Ti to form TiC and Ti_5Si_3, the mass ratio of SiC and Ti should be 3.2:1. Because the wettability between the TiC and Cu melts was very poor, a little more Ti has an advantage in the formation and dispersion of TiC. Therefore, the more accurate composition of the composites after the reaction of Ti–SiC to form TiC and Ti_5Si_3 would be Cu—3.7 vol.%, TiC—7.5 vol.%, Ti_5Si_3 and Cu—5.1 vol.%, TiC—10.3 vol.%, Ti_5Si_3 and Cu—7 vol.%, TiC—14.2 vol.% and Ti_5Si_3, respectively. According to our previous research [23], the Ti–SiC mixture will be immediately reacted after the addition into Cu melts, and the reaction products will be rapidly dispersed in the melts. The microstructures of the obtained as-cast composites are shown in Figure 1.

The microstructures of the TiC–Ti_5Si_3-reinforced Cu composites prepared by the melt reaction method combined with the traditional casting process are shown in Figure 1. It can be seen in Figure 1a,b that there seem to be three phases with different morphologies in the Cu matrix in the prepared Cu-4.86Ti-1Si-0.43C composite. The first one, which is marked as A in Figure 1b, is granular, with a size ranging from 1 μm to 6 μm, and the average mean is about 2 μm. Figure 2 shows the EDS analysis of the synthesized TiC and Ti_5Si_3 in the Cu-4.86Ti-1Si-0.43C sample. It can be seen in Figure 2b that the particles primarily include C and Ti elements, and the Ti/C atomic ratio is near 1:1. This result indicates that these particles are synthesized TiC particles. The second phase, marked as B in Figure 1b, which is acicular or claviform, mainly contains Ti and Si elements, as shown in Figure 2c. The atomic ratio of Ti and Si is about 1.67, demonstrating that it is the Ti_5Si_3 phase. The third phase, marked as D in Figure 1b, also seems to be granular, with an approximate size of 1~2 μm. However, it is noticed that, unlike the TiC particles, most of the D phase is not single-phase but consists of two phases. The magnified microstructure inserted in Figure 1b further confirmed that the D is a kind of the core–shell phase, with a thickness of the core ranging from about 100 nm to 500 nm. It is also found that the shell of the D phase is hexagonal, while the core is circular.

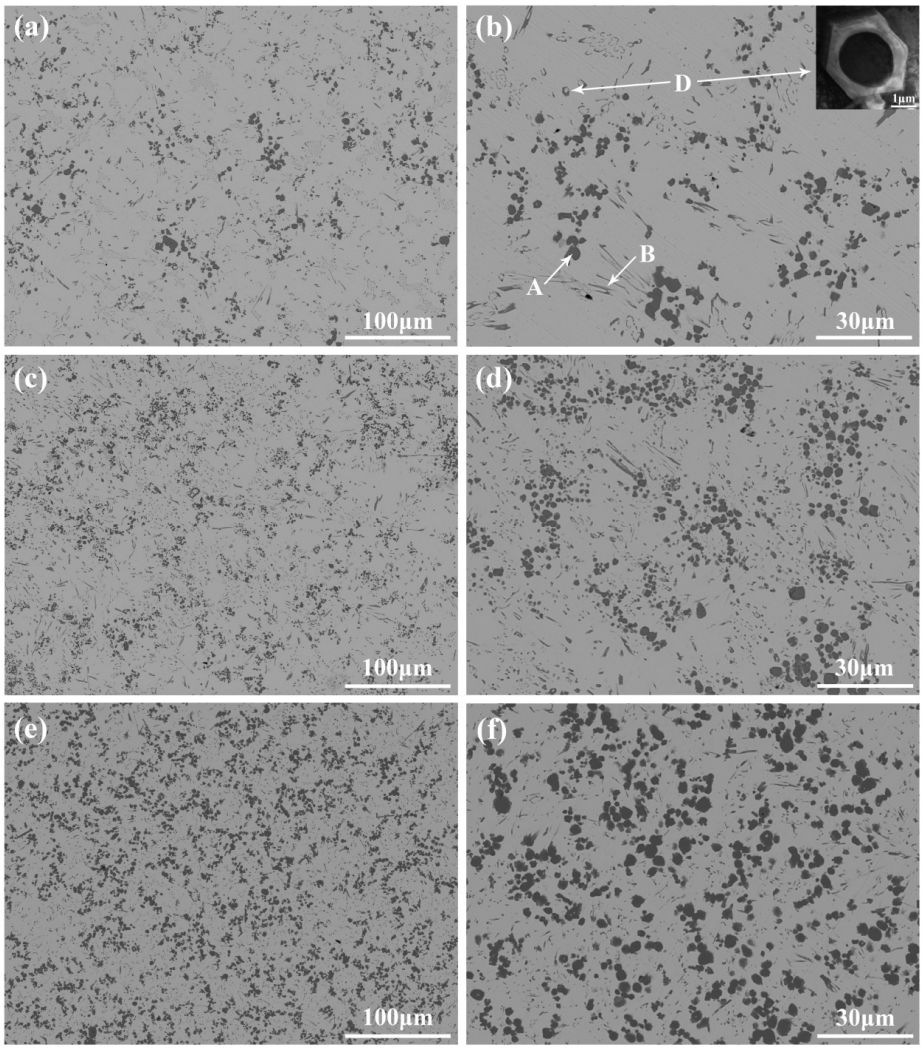

Figure 1. Microstructure of the as-cast composites prepared by Ti–SiC reaction in Cu melts. (**a**,**b**) Cu-4.86Ti-1Si-0.43C; (**c**,**d**) Cu-6.8Ti-1.4Si-0.6C; (**e**,**f**) Cu-9.72Ti-2Si-0.86C. (A-TiC; B-Ti_5Si_3; D-Cu@TixSiy).

Figure 2d shows the EDS line analysis results, which further prove that the shell of the D phase primarily includes Si and Ti, and the core is primarily Cu. Thus, it can be further proved that the D phase is the Cu@TixSiy phase, which has a core–shell structure.

Figure 3 displays the EDS mapping analysis results of the Ti_5Si_3 in prepared as-cast composites. The result of EDS mapping analysis further confirmed the above conclusion. It can be more clearly seen that the rod-like B phase and the shell of the D phase mainly consist of Ti and Si, while the core of the D phase is composed of the Cu element. The phase compositions of the prepared Cu-6.8Ti-1.4Si-0.6C and Cu-9.72Ti-2Si-0.86C composites are very similar to those of the Cu-4.86Ti-1Si-0.43C, as shown in Figure 1c–f. There are also three different morphology phases which are particle-like TiC, rod-like Ti_5Si_3 and the other particle-like phase with a core–shell structure. The differences are that, besides the formation of more TiC particles and Ti–Si compounds, the size of the more rod-like Ti_5Si_3 and TiC is also larger with the increase in Ti, Si and C contents. However, the increasing trend of size is not completely positively correlated with the content of Ti, Si and C. The mean size of TiC in Cu-6.8Ti-1.4Si-0.6C is about 1.6 μm, while it is about 2.58 μm in Cu-9.72Ti-2Si-0.86C.

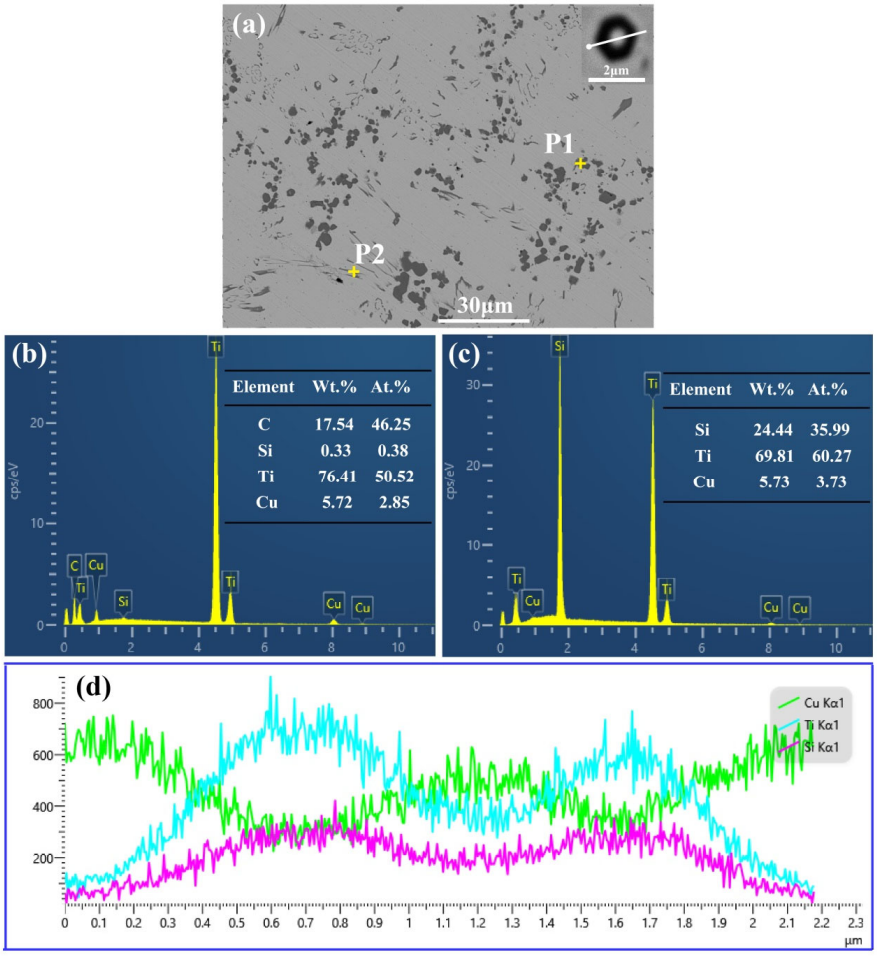

Figure 2. EDS analysis of the synthesized TiC and Ti_5Si_3 in the Cu-4.86Ti-1Si-0.43C sample. (**a**) The microstructure of the Cu-4.86Ti-1Si-0.43C sample; (**b**,**c**) EDS point analysis result of P1 and P2, respectively; (**d**) The EDS line analysis results of the Cu@Ti_xSi_y core–shell structure phase.

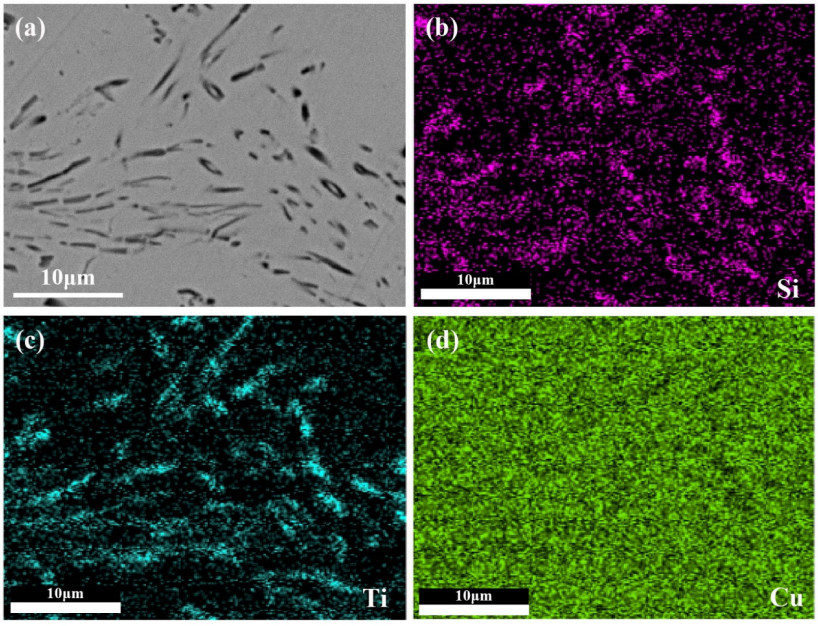

Figure 3. EDS mapping analysis of the Ti_5Si_3 in prepared as-cast composites. (**a**) Microstructures of the Ti_5Si_3 in prepared as-cast composites; (**b**–**d**) mapping micrographs of Si, Ti and Cu elements.

Figure 4 shows the XRD analysis results of the formed phases extracted from the as-cast composites. It is found that Ti and SiC were effectively introduced to promote the formation of TiC and Ti_5Si_3 in all the samples. In addition, there is no other kind of Ti–Si compound synthesized. These results demonstrate that the Ti–SiC mixtures have been completely reacted after adding them into the Cu melts. They also proved that the particle-like phase with a core–shell structure should be Cu@Ti_5Si_3.

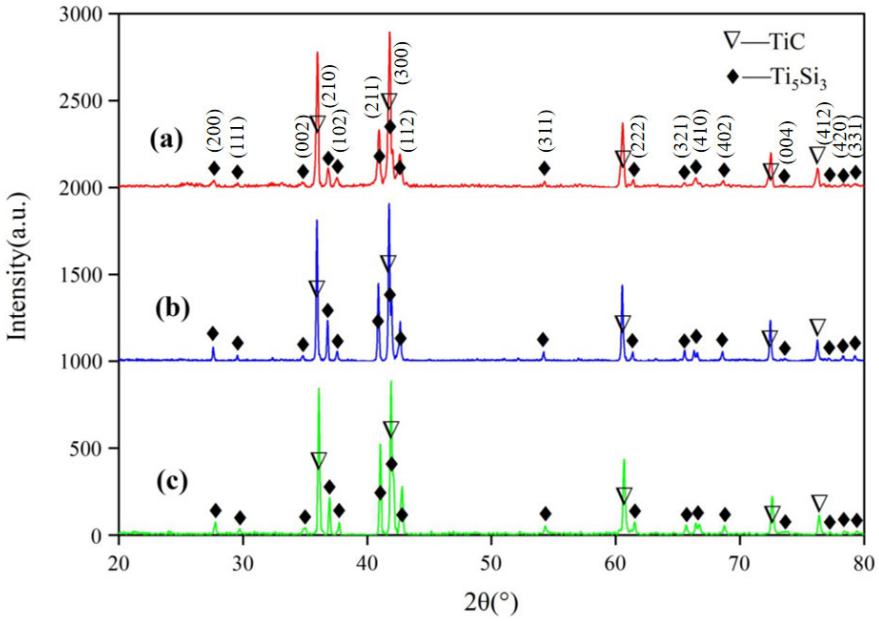

Figure 4. XRD patterns of the extracted powders from prepared composites. (**a**) Cu-4.86Ti-1Si-0.43C; (**b**) Cu-6.8Ti-1.4Si-0.6C; (**c**) Cu-9.72Ti-2Si-0.86C.

In order to further analyze the morphologies and the distribution of the reaction products, the as-cast composites are then deeply etched to remove the surface Cu matrix. The microstructures of the deeply etching samples are shown in Figure 5.

It can be seen in Figure 5a,b that, unlike the microstructure of the as-cast sample, there are only two phases with different morphologies in Cu-4.86Ti-1Si-0.43C. One is particle-like and the other is rod-like, and both of them are alternately distributed in the Cu matrix to form the hybrid reinforcement system together. The mean size of the particles is about 0.8 μm, while the diameter of the rod phase is about 1~2 μm, and the length-to-diameter ratio is about 5~25. Figure 6 shows the microstructures and EDS point analysis of the deeply etching samples. It can be seen from Figure 6c,e that the particles are TiC, and the EDS analysis results shown in Figure 6d,f also confirm that the rod phase is Ti_5Si_3 rods. In addition, it can be noted from Figure 5d that TiC particles are distributed in clusters, while Ti_5Si_3 rods, which are connected in a network structure, are distributed in clusters. The grid formed by Ti_5Si_3 clusters is filled with the Cu matrix, and each Ti_5Si_3 cluster is connected to form a spatial skeleton structure which is like a bird's nest. It can be seen in Figure 5a,b that the spatial structure of TiC and Ti_5Si_3 is not separately distributed, and many TiC particles stick to the Ti_5Si_3 rod.

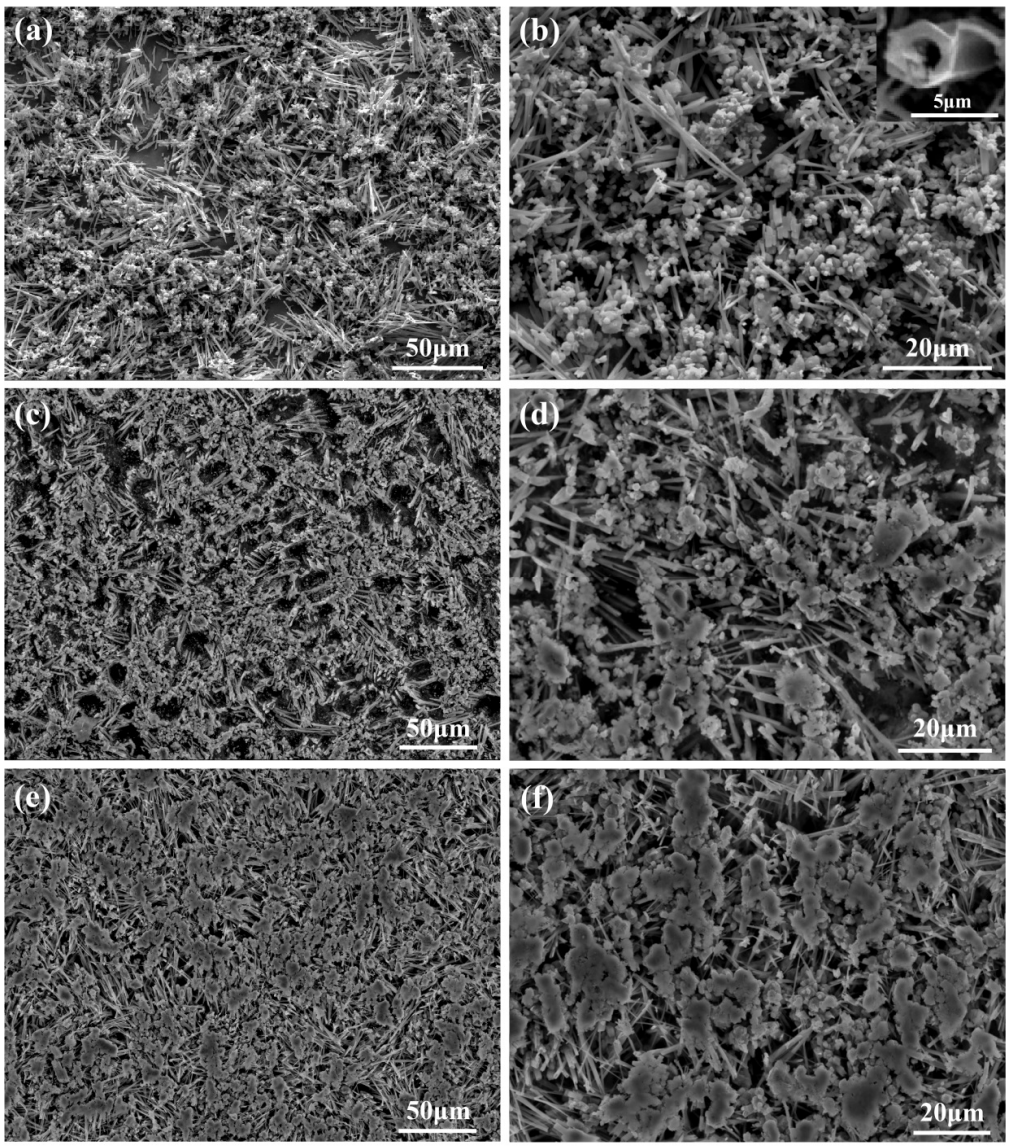

Figure 5. Microstructures of the deeply etching composites prepared by adding Ti–SiC with different contents. (**a**,**b**) Cu-4.86Ti-1Si-0.43C; (**c**,**d**) Cu-6.8Ti-1.4Si-0.6C; (**e**,**f**) Cu-9.72Ti-2Si-0.86C.

It is found that many Ti_5Si_3 rods are not solid but hollow, as the insert figure in Figure 5b shows. It can be seen that the hollow Ti_5Si_3 rod is a hexagonal prism with a cylindrical inner hole, whose cross-section is similar to the shell of the D phase shown in the insert figure in Figure 1b. It is deduced that those Ti_5Si_3 hollow rods should correspond to the core–shell particle-like D phase whose Cu cores have been completely etched away. The results further confirm that the core–shell phase is $Cu@Ti_5Si_3$. In addition, it is also demonstrated that the D phase, which seems to be particle-like in the as-cast sample, is actually rod-like. As a result, it can be concluded that all the Ti_5Si_3 have grown into the hexagonal prisms.

As for the Cu-6.8Ti-1.4Si-0.6C and Cu-9.72Ti-2Si-0.86C composites, it can be seen in Figure 5c–f that they also consist of TiC particles and Ti_5Si_3 rods. It is also noted that the TiC content of Cu-9.72Ti-2Si-0.86C is significantly greater than that of Cu-4.86Ti-1Si-0.43C, as shown in Figure 5a,e. The results prove that the content of TiC particles increases as the content of Ti–Si–C increases, and it is also found that more Ti_5Si_3 rods with a larger diameter and a smaller length-to-diameter ratio have been formed. It is deduced that those Ti_5Si_3 rods should correspond to the rod-like Ti_5Si_3 (B phase) present in the as-cast samples.

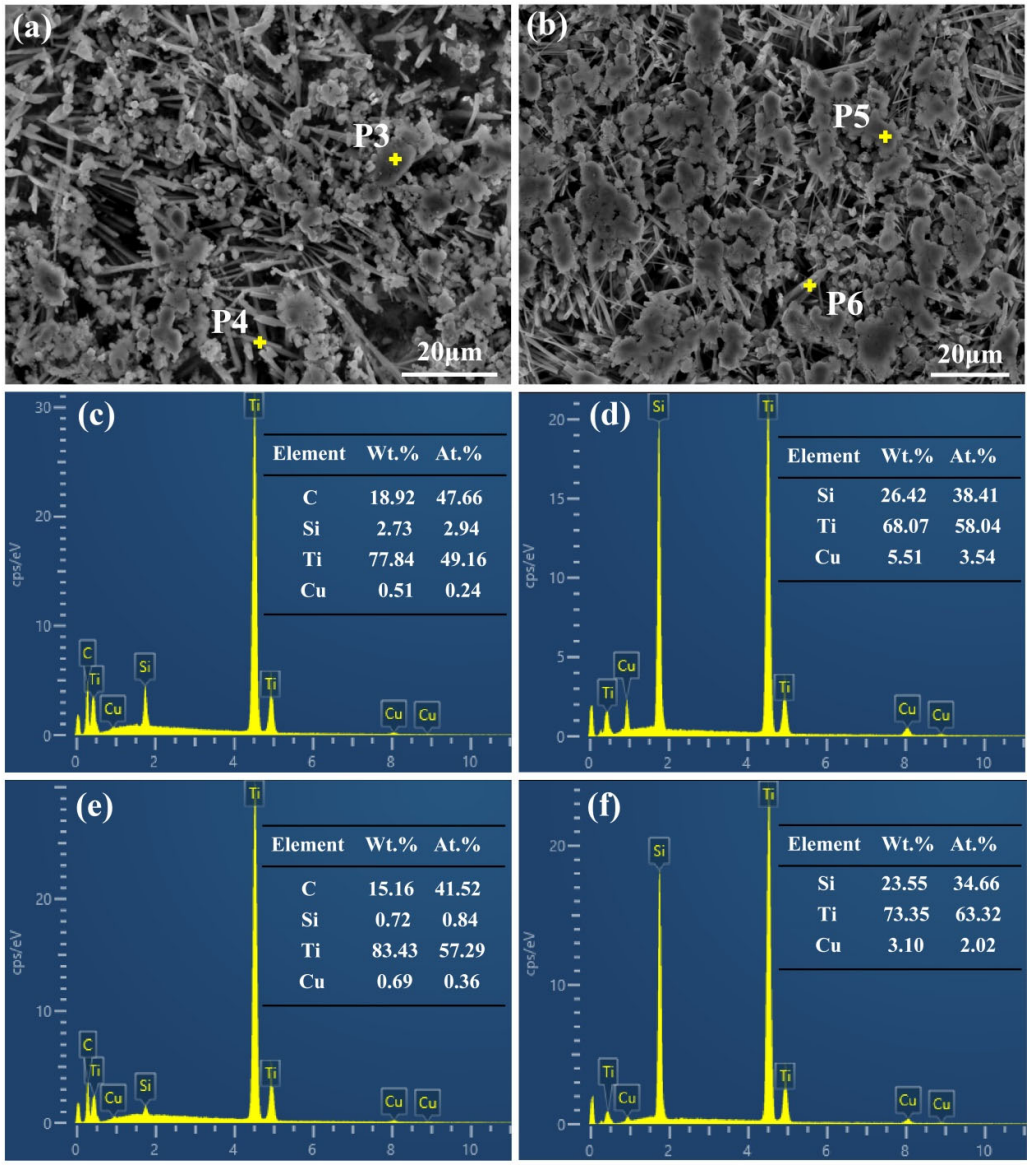

Figure 6. Microstructures and EDS point analysis of deeply etching samples. (**a**) Microstructures of Cu-6.8Ti-1.4Si-0.6C; (**b**) microstructures of Cu-9.72Ti-2Si-0.86C; (**c**–**f**) EDS point analysis result of P3, P4, P5 and P6, respectively (P3,P5-TiC; P4,P6-Ti_5Si_3).

According to the above results, it can be determined that Ti and SiC can be absolutely reacted in the Cu melts, and TiC and Ti_5Si_3 with different morphologies will be synthesized and alternately distributed. As a result, TiC particles and Ti_5Si_3 rods work together as reinforcements to form the hybrid reinforcement system. Regardless of the process, all the previous studies [23,24] suggested that Ti_5Si_3 is immediately formed in the Cu melts after Ti–SiC reaction. If so, it is deduced that the size of the Ti_5Si_3 should be significantly increased with the increase in Ti and Si content from Cu-4.86Ti-1Si-0.43C, Cu-6.8Ti-1.4Si-0.6C and Cu-9.72Ti-2Si-0.86C. Nevertheless, the results in this work show that the morphologies and sizes of Ti_5Si_3 are very similar in all samples. Therefore, it is deduced that the Ti_5Si_3 rods should not form in the melt during the holding time but rather crystallize from the melt during the solidification. It has been found in a previous work [25,26] that, like another D88 type of an orderly transition metal silicide, Mn_5Si_3, Ti_5Si_3 and Cu can form Cu–Ti_5Si_3 binary eutectic alloys. In the Cu melts, both primary and eutectic Ti_5Si_3 can grow into rod-like hexagonal prisms, which are the same as the Ti_5Si_3 synthesized in our prepared composites.

Hence, the more exact formation processes for TiC and Ti_5Si_3 by Ti–SiC reaction in Cu melts in this work should be as follows:

$$SiC + Ti \rightarrow Si(l) + TiC \quad (4)$$

where Si(l) is soluble Si. Then, during the solidification, Ti_5Si_3 is formed in two ways. One is directly crystalizing the melt to form the primary Ti_5Si_3; then, the remaining Ti and Si form the eutectic Ti_5Si_3 by the following eutectic reaction:

$$Cu + Ti(l) + Si(l) \rightarrow \alpha - Cu + Ti_5Si_3 \quad (5)$$

More primary Ti_5Si_3 will be formed by increasing the Ti and Si contents; thus, it is considered that the rod-like Ti_5Si_3 (B phase) shown in the as-cast samples is the primary Ti_5Si_3, while the other kind of Ti_5Si_3 (D phase) is the eutectic Ti_5Si_3.

As reported in previous works [26,27], the growth direction of the orderly transition metal silicide M5Si3, with a D88 crystal structure, is mainly determined by the periodic chain of the M–Si covalent bond due to its larger binding energy compared to that of Si–Si or M–M based on the Hartman–Perdok theory [28]. This is because the binding energy of the M–Si bond chain is greatest in the <0001> direction perpendicular to the base plane of (0001) due to the atomic arrangements with the shortest distance. As a result, the <0001> direction perpendicular to the base plane of (0001) is the fastest growing direction of all the directions, while, in the direction parallel to the base plane, the growth rate of the <1120> direction is greater than that of the other directions. As a result, M_5Si_3 crystals, such as Mn_5Si_3 and Ti_5Si_3, generally tend to grow into the rod-like hexagonal prism, which is in good agreement with the present work. As for the formation of core–shell prisms with Cu cores in Cu melts, a similar phenomenon is also present for the Mn_5Si_3 in brasses [26]. In addition, it is found that the Cu cores in the Cu@Ti_5Si_3 rods do not go through the whole rods but rather part of them, as shown in Figure 7a. Hence, as seen from the longitudinal section direction, the Ti_5Si_3 rods actually grow into H-shaped shells, and it can also be found that the end face of the Cu core in contact with Ti_5Si_3 is not flat but convex, corresponding to the concave Ti_5Si_3 inner end face. It can be inferred that both the D phase with a core–shell structure and the U-shaped shell in Figure 7b are part of the H-shaped shell [25].

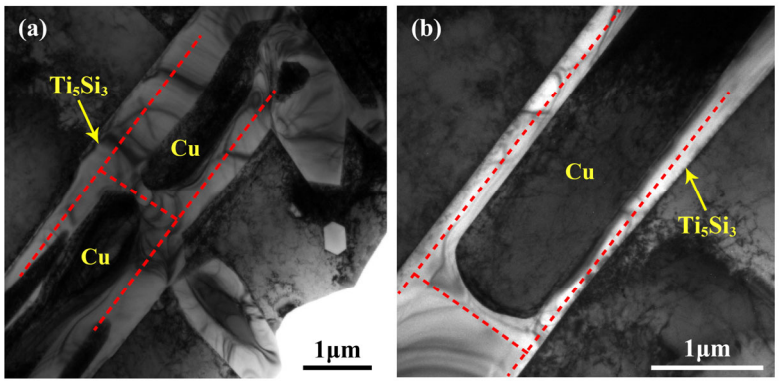

Figure 7. Microstructure of the longitudinal section direction of the core–shell structure Cu@Ti_5Si_3. (**a**) H-shaped; (**b**) U-shaped [25].

Figure 8 shows the growth processes of the core–shell structure Cu@Ti_5Si_3 in detail. According to the crystal growth characteristics and morphologies of Ti_5Si_3, it is considered that, in the early stage of Ti_5Si_3 formation, the hexagonal chip Ti_5Si_3 with (0001) as the base plane is first formed, as shown in Figure 8a. That will lead to the depletion of Ti and Si in the surrounding Cu melts, rapidly developing a solid hexagonal sheet, as shown in Figure 8b. Because of the fastest growth of the <0001> direction perpendicular to the (0001) base plane, the Ti and Si depletion along this direction will also be the worst. As a result, the following growth of Ti_5Si_3 along the <0001> direction will be mainly realized

by the horizontal diffusion of the surrounding Ti and Si atoms parallel to the (0001) plane. In this case, the growth of the inner region of the Ti_5Si_3 hexagonal prism will become more difficult than the outside region due to the longer diffusion distance. As a result, the cup-shaped structure will be formed, as shown in Figure 8c. The formation of the Ti_5Si_3 shell will further hinder the diffusion of Ti and Si from the outside to the inside. The formation of both the circular inner surface and the concave Ti_5Si_3 inner end face proves that the formation of Ti_5Si_3 shells is controlled by the horizontal diffusion of Ti and Si. At the beginning of the formation of the Ti_5Si_3 shell from the prism sheet, because the shell is very thin, it can only retard but not absolutely prevent the diffusion of Ti into the inner region. Now, the whole (0001) plane can still grow along the <0001> direction, but the closer it gets to the center, the slower it grows. Thus, the flat (0001) plane becomes concave, as shown in Figure 8c. Then, when the Ti_5Si_3 is high enough, Ti and Si will not be diffused from the outside to the inside at all, and the thickness of the Ti_5Si_3 will remain almost constant, as shown in Figure 8d. In the end, the H-shaped core–shell rods with cylindrical Cu cores are formed, as shown in Figure 8e. It is considered that the faster the growth rate along the <0001> direction, the thinner the Ti_5Si_3 shell will be. This can be confirmed by comparing the core–shell Ti_5Si_3 with the core–shell Mn_5Si_3 reported in Li's work [26]. It is found that the thickness of the shell in this work is much thinner than that in Mn_5Si_3. This should be due to the stronger bonding between Ti and Si, which will give rise to the much faster growth of the <0001> direction for Ti_5Si_3 compared to Mn_5Si_3.

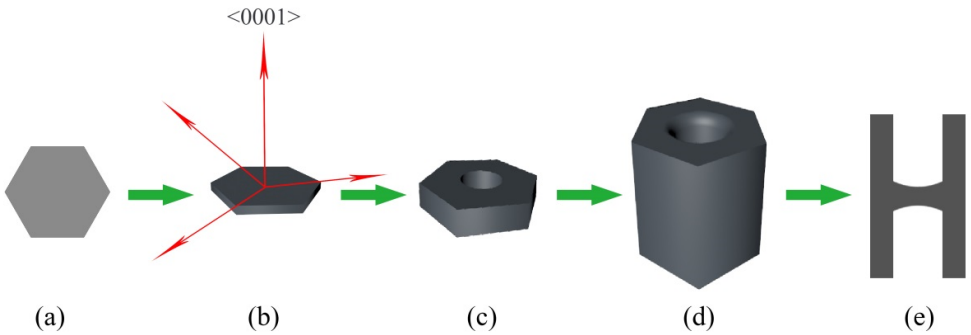

Figure 8. The growth processes of the core–shell structure Cu@Ti_5Si_3. (**a**) hexagonal chip; (**b**) solid hexagonal sheet; (**c**) cup-shaped structure; (**d**) hollow hexagonal prisms; (**e**) H-shaped core-shell rods.

Figure 9 shows the hardness of Cu and the composites prepared. It can be clearly seen that the hardness of the as-cast pure copper is only 62 HV, which is much lower than that of the prepared TiC–Ti_5Si_3 hybrid-reinforced Cu matrix composites. It should be noted that the hardness of the Cu-4.86Ti-1Si-0.43C composites is 136 HV, which is about 2.2 times that of the as-cast copper, and the hardness of the composites also tends to rise with the increase in the TiC–Ti_5Si_3 content. The hardness of the Cu-6.8Ti-1.4Si-0.6C and Cu-9.72Ti-2Si-0.86C composites is 150 HV and 170 HV, respectively, and the maximum hardness is 2.74 times that of the as-cast pure copper. The research [29] shows that TiC tends to agglomerate in the single TiC/Cu and influences the hardness of composites, and the hardness of Cu-10.68TiC is approximately 105 HV. Compared to the poor dispersion of TiC in TiC/Cu composites, TiC is more evenly distributed in the TiC–Ti_5Si_3 in situ-reinforced Cu composites due to the introduction of Ti_5Si_3. It is obvious that the addition of the TiC–Ti_5Si_3 hybrid-reinforced phase is more helpful for improving the hardness of pure copper. TiC and Ti_5Si_3 have different morphologies, which is beneficial for improving the properties of composites.

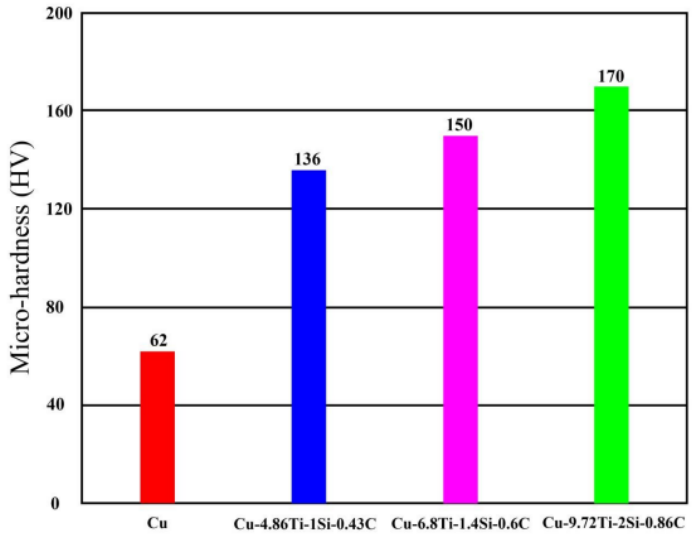

Figure 9. The hardness of the composites.

4. Conclusions

In summary, the TiC–Ti_5Si_3-reinforced Cu matrix composites were successfully prepared by reactive wetting based on the Ti–SiC system. Then, the microstructures of the TiC–Ti_5Si_3-reinforced Cu matrix composites were investigated. Finally, the hardness of the composites was tested. It is found that, in the prepared composites, TiC and Ti_5Si_3 alternately distribute in the Cu matrix to form the hybrid reinforcement system. The synthesized TiC is particle-like, with a size ranging from 0.5 μm to 3 μm, while the Ti_5Si_3 is a rod-like hexagonal prism with a diameter of about 1 μm and a length-to-diameter ratio of about 5~25. Many Ti_5Si_3 rods are core–shell structures, in which the shell is Ti_5Si_3, with a thickness of about 200 nm, and the core is Cu. With the increase in the Ti–SiC content, the TiC particles, Ti_5Si_3 rods and Cu@Ti_5Si_3 increased obviously, and the solid skeleton structure of TiC–Ti_5Si_3 was formed. The hardness of the composites was 2.2 to 2.74 times that of the as-cast pure copper. It is deduced that, compared to the composites reinforced by either TiC or Ti_5Si_3, the formation of the TiC–Ti_5Si_3 hybrid system is more helpful for improving the properties of the composites due to the different morphologies of TiC and Ti_5Si_3.

Author Contributions: Conceptualization, H.D.; methodology, H.D. and W.M.; validation, C.Z. and J.W.; investigation, F.Q.; writing—original draft preparation, C.Z.; writing—review and editing, X.Z. and J.Z.; funding acquisition, H.D. All authors have read and agreed to the published version of the manuscript.

Funding: This research was funded by the Natural Science Foundation of Beijing (No. 2232065), the Natural Science Foundation of Hebei Province (No. E2022502011), the Science and Technology Planning Project of Baoding Municipality (No. 2172P005), Pre-research Project (No. 80922020602) and the Fundamental Research Funds for the Central Universities (No. 2022MS092).

Institutional Review Board Statement: Not applicable.

Informed Consent Statement: Not applicable.

Data Availability Statement: The data supporting the findings of this study are available from the corresponding author, Haimin Ding, upon reasonable request.

Conflicts of Interest: The authors declare no conflict of interest.

References

1. Reza, S.; Mohammad, G.; Touradj, E.; Amir, H.P.; Ehsan, G. Preparation of Ag/reduced graphene oxide reinforced copper matrix composites through spark plasma sintering: An investigation of microstructure and mechanical properties. *Ceram. Int.* **2020**, *46*, 13569–13579. [CrossRef]
2. Ehsan, G.; Masoud, A.; Amir, H.P.; Touradj, E. Preparation of silicon carbide/carbon fiber composites through high-temperature spark plasma sintering. *J. Asian Ceram. Soc.* **2017**, *5*, 472–478. [CrossRef]
3. Madhesh, D.; Jagatheesan, K.; Sathish, T.; Balamanikandasuthan, K. Microstructural and Mechanical Properties of Copper Matrix Composites. *Mater. Today Proc.* **2021**, *37*, 1437–1441. [CrossRef]
4. Zhang, S.; Li, R.; Kang, H.; Chen, Z.; Wang, W.; Zou, C.; Li, T.; Wang, T. A High Strength and High Electrical Conductivity Cu-Cr-Zr Alloy Fabricated by Cryorolling and Intermediate Aging Treatment. *Mater. Sci. Eng. A* **2017**, *680*, 108–114. [CrossRef]
5. Ma, Y.; Lei, Q.; Cheng, J.; Gao, Y.; Meng, X.; Agbedor, S.O.; Xiao, Z. Microstructure and properties of a Cu-6Cr alloy with high friction and wear resistance. *Wear* **2023**, *514–515*, 204553. [CrossRef]
6. Han, L.; Liu, J.; Tang, H.; Yan, Z. Study of Zr addition on the composition, crystallite size, microstructure and properties of high-performance nano Cu alloys prepared by mechanical alloying. *Mater. Chem. Phys.* **2022**, *290*, 126630. [CrossRef]
7. Mukanov, S.; Loginov, P.; Fedotov, A.; Bychkova, M.; Antonyuk, M.; Levashov, E. The Effect of Copper on the Microstructure, Wear and Corrosion Resistance of CoCrCuFeNi High-Entropy Alloys Manufactured by Powder Metallurgy. *Materials* **2023**, *16*, 1178. [CrossRef]
8. Torabi, H.; Arghavanian, R. Investigations on the corrosion resistance and microhardness of Cu–10Sn/SiC composite manufactured by powder metallurgy process. *J. Alloys Compd.* **2019**, *806*, 99–105. [CrossRef]
9. Zhang, Y.; Choudhuri, D.; Scharf, T.W.; Descartes, S.; Chromik, R.R. Tribologically induced nanolaminate in a cold-sprayed WC-reinforced Cu matrix composite: A key to high wear resistance. *Mater. Des.* **2019**, *182*, 108009. [CrossRef]
10. Akbarpour, M.R.; Sadeghi, N.; Aghajani, H. Nano TiC-Graphene-Cu composites fabrication by a modified ball-milling method followed by reactive sintering: Effects of reinforcements content on microstructure, consolidation, and mechanical properties. *Ceram. Int.* **2022**, *48*, 130–136. [CrossRef]
11. Zhang, D.; He, X.; Liu, Y.; Bai, F.; Wang, J. The effect of in situ nano-sized particle content on the properties of TiCx/Cu composites. *J. Mater. Res. Technol.* **2021**, *10*, 453–459. [CrossRef]
12. Wang, Z.; Song, M.; Sun, C.; He, Y. Effects of particle size and distribution on the mechanical properties of SiC reinforced Al–Cu alloy composites. *Mater. Sci. Eng. A* **2011**, *528*, 1131–1137. [CrossRef]
13. Masroor, M.; Sheibani, S.; Ataie, A. Dispersion of Carbon Nanotubes in Cu-Cr Matrix Nano-composite by Wet Milling. *Procedia Mater. Sci.* **2015**, *11*, 560–564. [CrossRef]
14. Wang, B.; Zhang, H.; Yu, G.; Du, R.; He, P. A novel ultrasonic consolidation method for rapid preparation of diamond/Cu composites. *Mater. Lett.* **2022**, *323*, 132498. [CrossRef]
15. Zuo, H.; Wei, W.; Yang, Z.; Li, X.; Xie, W.; Liao, Q.; Xian, Y.; Ren, J.; Gao, G.; Wu, G. Synchronously improved mechanical strength and electrical conductivity of Carbon/Copper composites by forming Fe_3C interlayer at C/Cu interface. *Mater. Today Commun.* **2021**, *28*, 102661. [CrossRef]
16. Tian, W.; Zhou, D.; Qiu, F.; Jiang, Q. Superior tensile properties of in situ nano-sized TiCp/Al-Cu composites fabricated by reaction in melt method. *Mater. Sci. Eng. A* **2016**, *658*, 409–414. [CrossRef]
17. Qin, Y.; Tian, Y.; Peng, Y.; Luo, L.; Zan, X.; Xu, Q.; Wu, Y. Research status and development trend of preparation technology of ceramic particle dispersion strengthened copper-matrix composites. *J. Alloys Compd.* **2020**, *848*, 156475. [CrossRef]
18. Guo, L.; Yang, Y.; Wen, X.; Gao, H.; Wang, Z.; Guo, Z. Synthesis of Cu-based TiCx composites via in-situ reaction between CuxTi melt and dissolvable solid carbon. *Powder Technol.* **2020**, *362*, 375–385. [CrossRef]
19. Liu, Q.; Qi, F.; Wang, Q.; Ding, H.; Chu, K.; Liu, Y.; Li, C. The influence of particles size and its distribution on the degree of stress concentration in particulate reinforced metal matrix composites. *Mater. Sci. Eng. A* **2018**, *731*, 351–359. [CrossRef]
20. Wang, X.; Jie, J.; Liu, S.; Zhang, Y.; Li, T. Investigation of elastic modulus and morphology of reinforcement phase on the stress distribution of copper matrix composites. *J. Alloys Compd.* **2021**, *862*, 158532. [CrossRef]
21. Ding, H.; Chu, W.; Wang, Q.; Miao, W.; Wang, H.; Liu, Q.; Glandut, N.; Li, C. The In-Situ Synthesis of TiC in Cu Melts Based on Ti-C-Si System and Its Mechanism. *Mater. Des.* **2019**, *182*, 108007. [CrossRef]
22. Ding, H.; Wang, X.; Liu, Q.; Wang, J.; Li, C.; Zhang, X. The Stability and Transformation of TiC with Different Stoichiometries in Cu-Si Melts. *Mater. Des.* **2017**, *135*, 232–238. [CrossRef]
23. Ding, H.; Miao, W.; Chu, W.; Liu, Q.; Wang, J.; Chu, K.; Glandut, N.; Li, C. The Reaction Pathway of Ti-SiC System in Cu Melts. *J. Alloys Compd.* **2020**, *818*, 152860. [CrossRef]
24. Liu, Q.; Miao, W.; Ding, H.; Glandut, N.; Jia, H.; Li, C. The introduction of SiC into Cu melts based on Ti–SiC system and its transformation. *J. Mater. Res. Technol.* **2020**, *9*, 2881–2891. [CrossRef]
25. Liu, Q.; Zhang, X.; Wang, Q.; Miao, W.; Li, C.; Ding, H. Microstructure evolution of Ti_5Si_3 in Cu-Ti-Si alloys. *China Foundry* **2020**, *17*, 286–292. [CrossRef]
26. Li, H.; Jie, J.; Liu, S.; Zhang, Y.; Li, T. Crystal growth and morphology evolution of $D8_8$ $(Mn, Fe)_5Si_3$ phase and its influence on the mechanical and wear properties of brasses. *Mater. Sci. Eng. A* **2017**, *704*, 45–56. [CrossRef]
27. Yin, Y.; Wang, H. High-temperature wear behaviors of a laser melted Cuss/(Cr_5Si_3–CrSi) metal silicide alloy. *Mater. Sci. Eng. A.* **2007**, *452–453*, 746–750. [CrossRef]

28. Hartman, P.; Perdok, W.G. On the Relations Between Structure and Morphology of Crystals. I. *Acta Cryst.* **1955**, *8*, 521–524. [CrossRef]
29. Bagheri, G.H.A. The effect of reinforcement percentages on properties of copper matrix composites reinforced with TiC particles. *J. Alloys Compd.* **2016**, *676*, 120–126. [CrossRef]